



Perspectives in Magnetic Resonance

¹H-detected MAS solid-state NMR experiments enable the simultaneous mapping of rigid and dynamic domains of membrane proteinsT. Gopinath^a, Sarah E.D. Nelson^a, Gianluigi Veglia^{a,b,*}^a Department of Biochemistry, Molecular Biology, and Biophysics, University of Minnesota, Minneapolis, MN 55455, United States^b Department of Chemistry, University of Minnesota, Minneapolis, MN 55455, United States

ARTICLE INFO

Article history:

Received 28 June 2017

Revised 30 August 2017

Accepted 4 September 2017

Keywords:

Conformationally excited states

Simultaneous acquisitions

DUMAS

riHSQC

cpHSQC

Membrane proteins

ABSTRACT

Magic angle spinning (MAS) solid-state NMR (ssNMR) spectroscopy is emerging as a unique method for the atomic resolution structure determination of native membrane proteins in lipid bilayers. Although ¹³C-detected ssNMR experiments continue to play a major role, recent technological developments have made it possible to carry out ¹H-detected experiments, boosting both sensitivity and resolution. Here, we describe a new set of ¹H-detected hybrid pulse sequences that combine through-bond and through-space correlation elements into single experiments, enabling the simultaneous detection of rigid and dynamic domains of membrane proteins. As proof-of-principle, we applied these new pulse sequences to the membrane protein phospholamban (PLN) reconstituted in lipid bilayers under moderate MAS conditions. The cross-polarization (CP) based elements enabled the detection of the relatively immobile residues of PLN in the transmembrane domain using through-space correlations; whereas the most dynamic region, which is in equilibrium between folded and unfolded states, was mapped by through-bond INEPT-based elements. These new ¹H-detected experiments will enable one to detect not only the most populated (ground) states of biomacromolecules, but also sparsely populated high-energy (excited) states for a complete characterization of protein free energy landscapes.

© 2017 Elsevier Inc. All rights reserved.

1. Introduction

Solid-state NMR (ssNMR) is the method of choice for probing structure, dynamics, chemistry, and ligand binding of microcrystalline, membrane-bound, and fibrillar proteins with atomic resolution [1–4]. Sensitivity and resolution of the resonances in multidimensional NMR spectra are fundamental requirements for protein structural analysis. Recent reviews have illustrated the most important achievements in this field [5–8]. These advancements are due to developments in high-field magnet technology, probe design, isotopic-labeling schemes, improved sample preparation techniques, and modern pulse sequences. However, the sensitivity and resolution of the ssNMR spectra still limit the routine application of these techniques for membrane proteins, where lipids are essential in sample preparations to maintain native conditions.

In recent years, our group has been redesigning the classical MAS ssNMR experiments for resonance assignment and distance determination in biological solids, boosting both sensitivity and

resolution [9–12]. Toward this goal, we developed a new class of experiments called Polarization Optimized Experiments (POE) that utilize orphan spin operators to generate up to eight multidimensional NMR spectra from one pulse sequence [9,13]. These experiments are performed using commercial ssNMR probes for bio-solids and require only one receiver. POE methodology exploits simultaneous cross-polarization (CP) and long-lived ¹⁵N polarization of isotopically labeled proteins for generating multiple acquisitions. Recently, POE have been extended to ¹H detection under moderate or fast MAS conditions using perdeuterated sample preparations to further improve their sensitivity [14–18].

As for soluble proteins, integral or membrane-associated proteins populate different structural states modulated by their lipid environment as well as conformational dynamics [19–21]. Conformational dynamics can promote proteins' to alternate states, characterized by high conformational energy, often referred to as conformationally excited states. These states are sparsely populated and have been found to play an essential role in many biological functions [20–22]. However, detecting these lowly populated dynamic states using ¹³C detected experiments and conventional CP-based ssNMR pulse sequences is quite challenging. In fact, fast motions of protein segments can dramatically scale down anisotropic NMR interactions such as chemical shift anisotropy and dipolar

* Corresponding author at: Department of Biochemistry, Biophysics, and Molecular Biology, University of Minnesota, 6-155 Jackson Hall, MN 55455, United States.
E-mail address: vegli001@umn.edu (G. Veglia).

couplings [23–25]. These effects increase the coherences lifetime (T_2), and have enabled the detection of mobile domains using solution-NMR type pulse sequences under moderate spinning speeds [26,27]. Following a similar strategy, we recently described ^1H detected through-bond correlation experiments for studying conformationally excited states of membrane proteins under moderate MAS conditions using fully protonated samples reconstituted in hydrated proteoliposomes [28]. These experiments were successfully applied to phospholamban (PLN), a cardiac membrane protein that regulates calcium transport across the sarcoplasmic reticulum (SR) membrane by interacting with the sarcoplasmic reticulum Ca^{2+} -ATPase (SERCA) [20]. We demonstrated that a sensitivity enhancement of up to ten times can be achieved via ^1H -detected ^{15}N HSQC type MAS experiments. Notably, these highly sensitive ^1H detected experiments allowed us to detect weakly populated (less than 5%) excited states of phospholamban in various lipid mixtures [28]. Therefore, a complete structural analysis of the different functional states of membrane proteins may require the application of both INEPT and CP-based experiments [29,30].

In this work, we report a new strategy for ^1H detected experiments on membrane proteins. We showed that it is possible to acquire both INEPT- and CP-based 2D correlation spectra in a single experiment. Specifically, we were able to image both N-H^{N} and $\text{C}\alpha\text{-H}^{\text{N}}$ fingerprints detecting both the ground and the excited states of PLN, speeding up the characterization of the conformational energy landscape for membrane proteins.

2. Material and methods

Uniformly $^{13}\text{C}/^{15}\text{N}$ labeled monomeric PLN (PLN^{AFA}) was expressed as a fusion protein with maltose binding protein in BL21 (DE3) *E. coli* and purified as reported previously [31]. The final sample consisting of about 2 mg of PLN was reconstituted in 1:100 protein to lipid ratio with DMPC liposomes and packed into a 3.2 mm Agilent MAS rotor using a series of centrifugation steps [20]. All of the solid-state NMR experiments were acquired at the Minnesota NMR center using an Agilent ssNMR spectrometer operating at a ^1H Larmor frequency of 600 MHz and equipped with 3.2 mm MAS probe with reduced RF heating technology. MAS rate of 12 kHz was used in all the experiments with a recycle delay of 3 s and 50 kHz spectral width in the t_2 dimension. For immobile regions of membrane proteins that are detectable via CP-based experiments, the transverse relaxation times (T_2) are relatively short. For this reason, the t_1 and t_2 evolution periods are relatively short for the cpHSQC compared to the INEPT-based riHSQC experiment. In our experiments, the number of t_1 increments for riHSQC and cpHSQC were set to 80 and 40, with a dwell time of 200 μs that gives maximum t_1 evolution periods of 16 and 8 ms, respectively. Two loops were applied ($n = 2$, see Fig. 1B and C) during the t_1 evolution of cpHSQC, where each t_1 loop with 40 increments was processed separately and then added for obtaining the final cpHSQC spectrum. A similar strategy was previously applied to obtain dual acquisition spectra in the DUMAS and MEIOSIS methods [9,10]. The t_2 acquisition time was set to 30 and 20 ms for riHSQC and cpHSQC experiments, respectively.

The 90° pulse lengths for ^1H , ^{13}C , and ^{15}N were set to 2.5, 7, and 7 μs , respectively. Water suppression was obtained from phase switched spin-lock pulses with phases x and y with RF amplitude of 30 kHz and duration (τ_1) set to 200–250 ms. For riHSQC experiments, the τ value was set to 5.4 ms ($1/2 J_{\text{NH}}$), and during t_2 acquisition ^{15}N heteronuclear decoupling was obtained using the WALTZ-16 sequence with the RF amplitude set to 10 kHz [32]. For cpHSQC, during ^1H - ^{13}C or ^{15}N - ^1H CP transfer ^{13}C , ^{15}N and ^1H RF amplitudes were set to 35, 35 and 59 kHz respectively, while the ^1H RF amplitude was linearly ramped from 80 to 100%. The

optimal Hartmann–Hahn (HH) contact time for ^1H - ^{15}N or ^1H - ^{13}C CP was found to be 500–1000 μs at different temperatures, whereas the length of ^1H - ^{15}N -CP prior to acquisition was set to 200 μs for selective N-H^{N} transfer. During ^{15}N or ^{13}C t_1 evolution, TPPM decoupling was applied on ^1H with 100 kHz RF amplitude. For the specific-CP transfer from $^{13}\text{C}\alpha$ (^{13}CO) to ^{15}N , 100 kHz CW decoupling was applied on ^1H , whereas ^{15}N RF amplitude was set to $(5/2)\cdot\omega_r$ (~ 29.5 kHz), and ^{13}C RF amplitude was set to $(3/2)\cdot\omega_r$ (~ 18.6 kHz) and $(7/2)\cdot\omega_r$ (~ 41 kHz) for $^{13}\text{C}\alpha$ and ^{13}CO specific-CP, respectively. The specific-CP was implemented with an adiabatic ramp ($\Delta \sim 1.6$ kHz and $\beta = 0.5$ kHz), and the contact times for CAN and CON transfers were set to 3.0 and 3.3 ms, respectively. During t_2 ^1H acquisition of cpHSQC experiments a window-PMLG (phase modulated Lee-Goldberg) was applied on the ^1H channel [33]. The window acquisition parameters were optimized on a standard $\text{U-}^{13}\text{C}$, ^{15}N NAVL (N-acetyl-Valine-Leucine) sample, where the ^1H line widths were found to be between 120 and 150 Hz. In each cycle of window-PMLG, a detection period of 1.8 μs was inserted between 1.3 and 0.8 μs delay periods that account for receiver and probe ringing, followed by m5m PMLG sequence with RF amplitude of 100 kHz and length 14 μs . All the spectra were processed using NMRPipe [34] and analyzed using Sparky [35–37].

3. Results

When applied to a given membrane protein, the riHSQC and cpHSQC pulse sequences map N-H^{N} backbone fingerprints of dynamic and immobile residues, respectively. The ^1H detected riHSQC pulse sequence consists of water suppression (τ_1) and t_1 evolution periods that are sandwiched between two ^1H - ^{15}N refocused INEPT periods (Fig. 1A). In the cpHSQC pulse sequence (Fig. 1B), on the other hand, water suppression and t_1 evolution periods are sandwiched between two ^1H - ^{15}N CP periods followed by ^1H detection under window PMLG sequence. The window PMLG sequence improves the ^1H line widths significantly by suppressing homonuclear dipolar couplings. A significant drawback of window acquisition is the reduced sensitivity due to limited detection points. However, under fast MAS conditions, it is possible to recover both sensitivity and resolution using regular acquisition.

To make the best of nuclear spin polarization and reduce the experimental time, we combined riHSQC and cpHSQC pulse sequences into single experiments. We propose two new schemes (Fig. 1C and D) that include two acquisition periods per each scan and record riHSQC and cpHSQC in first and second acquisitions, respectively. In the pulse sequence represented in Fig. 1C, the polarization is initially transferred from ^1H to ^{13}C using CP followed by a 90° pulse that creates ^{13}C z-magnetization. The riHSQC pulse sequence is then applied on ^1H and ^{15}N channels while storing the ^{13}C polarization along z-direction. After the first acquisition, the carbonyl magnetization is transferred to ^{15}N via specific-CP followed by a t_1 evolution period. A short ^1H - ^{15}N CP (~ 150 – 200 μs) is then applied for selective polarization transfer from the ^{15}N nuclei to the directly bonded amide protons followed by ^1H detection during the second acquisition. Note that during riHSQC sequence and its t_1 evolution, the ^{13}C z-spin operator undergoes T_1 relaxation. In order to keep the relaxation constant for all t_1 increments, a delay of $(\text{CT}-t_1)$ is applied at the end of first acquisition. Fig. 1D shows another version of the pulse sequence, where the riHSQC is acquired during the first acquisition followed by a 90° pulse on ^{13}C that creates ^{13}CO direct polarization that is used for recording cpHSQC during the second acquisition. In conventional cpHSQC (Fig. 1B), the polarization follows the H-N-H^{N} pathway; whereas for the cpHSQC acquired in second acquisition the polarization follows the $\text{H-CO-N}^{\text{N}}\text{H}$ and $\text{CO-N}^{\text{N}}\text{H}$ pathways, respectively (Fig. 1C and D).

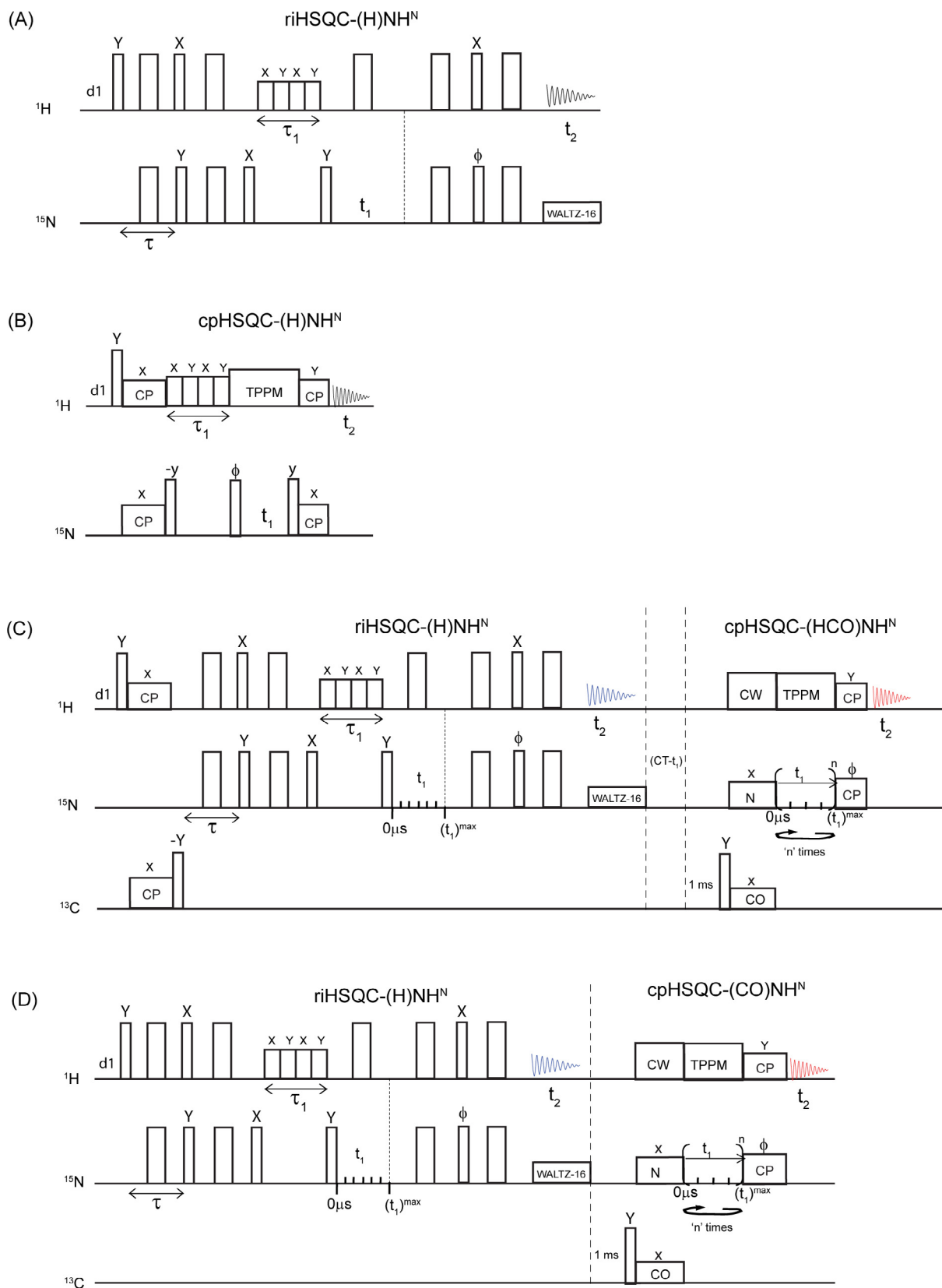


Fig. 1. Pulse sequences for two-dimensional ^1H -detected cpHSQC and riHSQC two-dimensional experiments for mapping N-H^{N} backbone finger prints of ground and excited states of proteins. (A) riHSQC, (B) cpHSQC pulse sequences using single acquisition. (C) and (D) show new pulse sequences for simultaneous acquisition of riHSQC and cpHSQC in first and second acquisitions respectively. The t_1 evolution was used with two loops ($n = 2$) for cpHSQC prior to second acquisition. For all the pulse sequences, a two-step phase cycle was used by switching the ϕ and receiver phases, t_1 states acquisition was obtained by altering the phase of ϕ pulse between x and y.

We applied the ^1H detected HSQC experiments on U- ^{13}C , ^{15}N labeled phospholamban (PLN), a 52-residue membrane protein that regulates the SR Ca^{2+} -ATPase. PLN comprises an inhibitory transmembrane domain (domain Ib and domain II) and a regulatory domain (domain Ia), connected by a short, flexible loop. Fig. 2 compares the sensitivity of riHSQC and cpHSQC 1D spectra acquired using single and dual acquisition methods, respectively. The sensitivity for the riHSQC is almost identical between the two methods; whereas the sensitivity of cpHSQC acquired using the dual acquisition method is $\sim 50\%$ lower compared to single acquisition sequence. The sensitivity achieved in 'n' scans is \sqrt{n} , so the sensitivity in 'n/4' scans is equal to $\sqrt{n/4}$ or $0.5 * \sqrt{n}$ which is equal to half of the sensitivity. In other words, the cpHSQC acquired separately would require about one fourth of the number scans ($\sim 25\%$ more experimental time), hence, the dual acquisition sequences result in a time saving of $\sim 25\%$. Indeed, a loss of signal is expected for the cpHSQC sequence as the additional polarization transfer pathways as well ^{13}C T_1 relaxation reduces the initial ^{15}N polarization prior to the t_1 evolution period. Nevertheless, the

cpHSQC spectrum is acquired along with riHSQC with almost no additional time. This sensitivity comparison is also shown for the 2D spectra in Fig. 3. The riHSQC of Fig. 3A and cpHSQC of Fig. 3B were acquired in 23.52 and 6.1 h, respectively, whereas Fig. 3C shows the simultaneous acquisition of both the spectra using 24.08 h. Integrated intensity of riHSQC and cpHSQC were found to be almost similar between Fig. 3A, B, and C, with a 25% time saving using the dual acquisition. Previous solution and solid-state NMR as well electron paramagnetic resonance (EPR) experiments from our group and others have shown that PLN's regulatory region in the absence of SERCA undergoes a conformational equilibrium between an ordered T state (helical) and a disordered R state (unfolded and membrane detached) [27,38]. The red envelop of peaks correspond to the most rigid resonances (T-state + inhibitory domain) of the protein, while the resonances in blue correspond to the most dynamic region of the protein (domain Ia and loop) which correspond to the disordered R-state (see Fig. 3C). The schematic of T and R-state equilibrium is shown in Fig. 3D (PDB structures 2KB7 and 2LPF), where the domains Ia, Ib and loop regions are highlighted in blue.

The pulse sequences for simultaneous acquisition ^{15}N -edited riHSQC and cpHSQC of Fig. 1C and D, can also be extended to ^{13}C edited experiments. Fig. 4A shows another example where the first acquisition records ^{15}N -edited sensitivity enhanced riHSQC (SE-riHSQC) experiment [28]; whereas second acquisition utilizes a direct $\text{C}\alpha$ polarization for CA(N)H $^{\text{N}}$ correlation via CA-N and N-H polarization transfer periods. The 2D ^{15}N -edited riHSQC and $^{13}\text{C}\alpha$ edited cpHSQC spectra of PLN are shown in Fig. 4B. Note that the ^1H resolution in the ^{15}N -edited cpHSQC (Fig. 3) is similar to that of the ^{13}C -edited cpHSQC (Fig. 4B). The t_2 for the detection of the

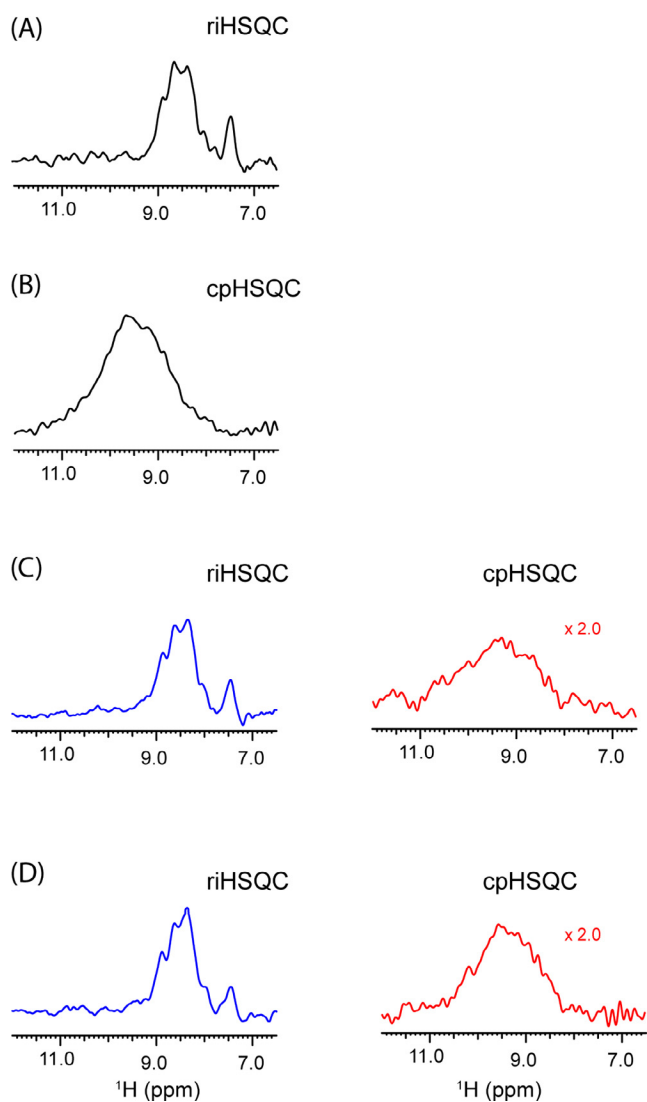


Fig. 2. Phospholamban amide ^1H spectra obtained from riHSQC and cpHSQC experiments by using the pulse sequences of Fig. 1 with t_1 set to zero. (A) and (B) were respectively acquired using riHSQC and cpHSQC shown in Fig. 1A and B. Each of the two spectra in (C) and (D) were simultaneously acquired by using the pulse sequences of Fig. 1C and D respectively.

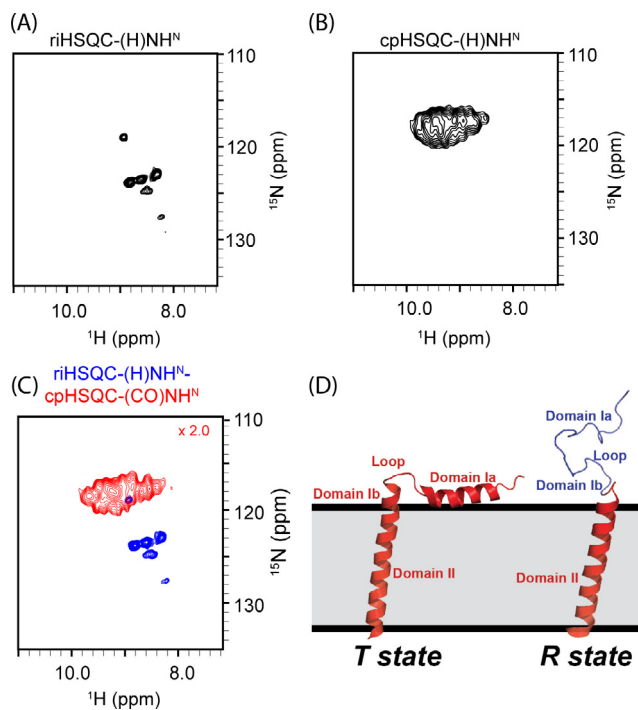


Fig. 3. 2D N-H $^{\text{N}}$ correlation spectra of phospholamban membrane protein obtained from the pulse sequences of Fig. 1. The spectra in (A) and (B) were acquired separately using the pulse sequences of Fig. 1A and B respectively. (C) 2D spectra riHSQC (blue) and cpHSQC (red) were simultaneously acquired using the pulse sequence of Fig. 1D. The riHSQC spectrum maps the dynamic cytoplasmic residues of phospholamban, whereas the relatively immobile transmembrane and juxtamembrane residues are mapped by the cpHSQC spectrum. (D) Structures of PLN in the T (2KB7) and R (2LPF) states. (For interpretation of the references to colour in this figure legend, the reader is referred to the web version of this article.)

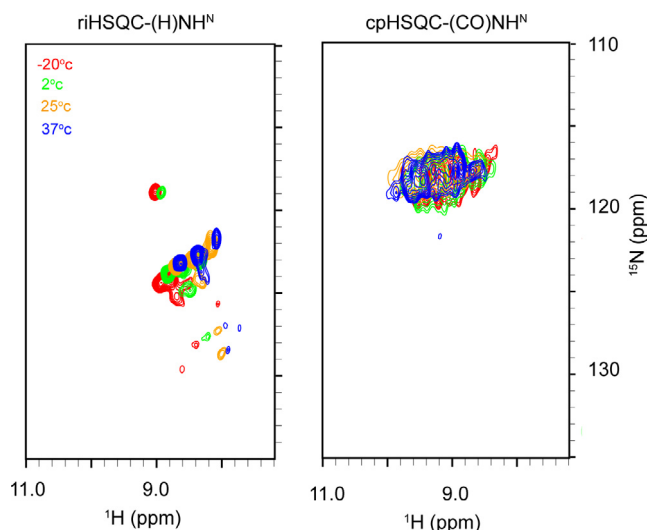


Fig. 5. Simultaneous acquisition of riHSQC and cpHSQC spectra of phospholamban using the pulse sequence of Fig. 1D at different temperatures. The relative peak positions of cpHSQC spectra remain similar, whereas the riHSQC peaks are gradually shifted as a function of temperature indicating the change in structural dynamics.

excited states simultaneously and make it possible to have a semi quantitative estimate of the conformational equilibrium and the energy landscape of PLN. Although the co-existence of T and R-state were already demonstrated in our previous publications using ^{13}C detected experiments [20,27], the complete assignment of R state residues was not possible due to a low sensitivity of the samples. The highly sensitive ^1H -detected methods will enable the acquisition of 3D sequential correlation experiments for mapping of the R-state residues of the cytoplasmic region. Recently, we have demonstrated the quantification of relative populations of the T and R states using ^{15}N detection (1D CP and rINEPT experiments) [28]. In principle, ^1H detection (1D cpHSQC and riHSQC experiments) could be used for estimating these populations. However, the length of the ^1H detected experiments is twice that of ^{15}N detected experiments and the spin dynamics is different due to the strong ^1H - ^1H dipolar interactions, preventing an accurate quantification. The latter is exacerbated by the long water suppression element that is necessary for ^1H detected experiments. While for crystalline and amyloid proteins, water suppression is usually achieved using short spin lock periods (τ_1) of 50–100 ms, in our experiments τ_1 needs to be set to 200–250 ms due to the higher water content of lipid-based membrane protein samples. Also, the ^1H line widths of cpHSQC experiments at 12 kHz MAS are relatively broad compared to crystalline proteins in spite of using homonuclear window-PMLG decoupling. We anticipate that the application of these pulse sequences under fast MAS conditions (40–60 kHz) can further improve the line widths as well as sensitivity. Although the current experiments were demonstrated using a regular MAS setup (without gradient and field lock channels) a further gain in both sensitivity and resolution will be possible, thanks to these technological advancements.

5. Conclusions

In conclusion, we have developed a new ^1H -detection strategy for simultaneous acquisition of CP- and INEPT-based out-and-back experiments on membrane proteins, which resulted in approximately 25% time saving. We successfully tested these new pulse sequences on fully protonated U- ^{13}C , ^{15}N labeled PLN in proteoliposomes using 12 kHz MAS spinning rate. These new

methods provide the basis for the development of 3D sequential correlation experiments for detecting and characterizing both ground and excited states of membrane proteins embedded in biologically relevant lipid membrane models.

Acknowledgments

This work is supported by the National Institutes of Health (GM 64742 and GM 72701). The NMR experiments were carried out at the Minnesota NMR Center.

References

- [1] F. Castellani, B. van Rossum, A. Diehl, M. Schubert, K. Rehbein, H. Oschkinat, Structure of a protein determined by solid-state magic-angle-spinning NMR spectroscopy, *Nature* 420 (2002) 98–102.
- [2] F. Hu, W. Luo, M. Hong, Mechanisms of proton conduction and gating in influenza M2 proton channels from solid-state NMR, *Science* 330 (2010) 505–508.
- [3] A. McDermott, Structure and dynamics of membrane proteins by magic angle spinning solid-state NMR, *Annu. Rev. Biophys.* (2009) 385–403.
- [4] E.D. Watt, C.M. Rienstra, Recent advances in solid-state nuclear magnetic resonance techniques to quantify biomolecular dynamics, *Anal. Chem.* 86 (2014) 58–64.
- [5] S. Wang, V. Ladizhansky, Recent advances in magic angle spinning solid state NMR of membrane proteins, *Prog. Nucl. Magn. Reson. Spectrosc.* 82C (2014) 1–26.
- [6] Y. Miao, T.A. Cross, Solid state NMR and protein-protein interactions in membranes, *Curr. Opin. Struct. Biol.* 23 (2013) 919–928.
- [7] S.J. Opella, Relating structure and function of viral membrane-spanning miniproteins, *Curr. Opin. Virol.* 12 (2015) 121–125.
- [8] S.J. Opella, Solid-state NMR and membrane proteins, *J. Magn. Reson.* 253 (2015) 129–137.
- [9] T. Gopinath, G. Veglia, Dual acquisition magic-angle spinning solid-state NMR-spectroscopy: simultaneous acquisition of multidimensional spectra of biomacromolecules, *Angew. Chem.* 51 (2012) 2731–2735.
- [10] T. Gopinath, G. Veglia, Orphan spin operators enable the acquisition of multiple 2D and 3D magic angle spinning solid-state NMR spectra, *J. Chem. Phys.* 138 (2013) 184201.
- [11] T. Gopinath, G. Veglia, Orphan spin polarization: a catalyst for high-throughput solid-state NMR spectroscopy of proteins, *Annu. Rep. NMR Spectrosc.* 89 (2016) 103–121.
- [12] K.R. Mote, T. Gopinath, G. Veglia, Determination of structural topology of a membrane protein in lipid bilayers using polarization optimized experiments (POE) for static and MAS solid state NMR spectroscopy, *J. Biomol. NMR* 57 (2013) 91–102.
- [13] T. Gopinath, G. Veglia, Multiple acquisitions via sequential transfer of orphan spin polarization (MAeSTOSO): how far can we push residual spin polarization in solid-state NMR?, *J. Magn. Reson.* 267 (2016) 1–8.
- [14] B. Reif, Ultra-high resolution in MAS solid-state NMR of perdeuterated proteins: implications for structure and dynamics, *J. Magn. Reson.* 216 (2012) 1–12.
- [15] L.B. Andreas, T. Le Marchand, K. Jaudzems, G. Pintacuda, High-resolution proton-detected NMR of proteins at very fast MAS, *J. Magn. Reson.* 253 (2015) 36–49.
- [16] P. Bellstedt, C. Herbst, S. Hafner, J. Leppert, M. Gorch, R. Ramachandran, Solid state NMR of proteins at high MAS frequencies: symmetry-based mixing and simultaneous acquisition of chemical shift correlation spectra, *J. Biomol. NMR* 54 (2012) 325–335.
- [17] B.B. Das, S.J. Opella, Simultaneous cross polarization to ^{13}C and ^{15}N with ^1H detection at 60kHz MAS solid-state NMR, *J. Magn. Reson.* 262 (2016) 20–26.
- [18] K. Sharma, P.K. Madhu, K.R. Mote, A suite of pulse sequences based on multiple sequential acquisitions at one and two radiofrequency channels for solid-state magic-angle spinning NMR studies of proteins, *J. Biomol. NMR* 65 (2016) 127–141.
- [19] D.M. Korzhnev, X. Salvatella, M. Vendruscolo, A.A. Di Nardo, A.R. Davidson, C. M. Dobson, L.E. Kay, Low-populated folding intermediates of Fyn SH3 characterized by relaxation dispersion NMR, *Nature* 430 (2004) 586–590.
- [20] M. Gustavsson, R. Verardi, D.G. Mullen, K.R. Mote, N.J. Traaseth, T. Gopinath, G. Veglia, Allosteric regulation of SERCA by phosphorylation-mediated conformational shift of phospholamban, *Proc. Natl. Acad. Sci. USA* 110 (2013) 17338–17343.
- [21] R. Briones, C. Weichbrodt, L. Paltrinieri, I. Mey, S. Villinger, K. Giller, A. Lange, M. Zweckstetter, C. Griesinger, S. Becker, C. Steinem, B.L. de Groot, Voltage dependence of conformational dynamics and subconducting states of VDAC-1, *Biophys. J.* 111 (2016) 1223–1234.
- [22] G. Kar, O. Keskin, A. Gursoy, R. Nussinov, Allostery and population shift in drug discovery, *Curr. Opin. Pharmacol.* 10 (2010) 715–722.
- [23] O.C. Andronesi, S. Becker, K. Seidel, H. Heise, H.S. Young, M. Baldus, Determination of membrane protein structure and dynamics by magic-angle-spinning solid-state NMR spectroscopy, *J. Am. Chem. Soc.* 127 (2005) 12965–12974.

- [24] U.H. Durr, K. Yamamoto, S.C. Im, L. Waskell, A. Ramamoorthy, Solid-state NMR reveals structural and dynamical properties of a membrane-anchored electron-carrier protein, cytochrome b5, *J. Am. Chem. Soc.* 129 (2007) 6670–6671.
- [25] G. Fusco, A. De Simone, T. Gopinath, V. Vostrikov, M. Vendruscolo, C.M. Dobson, G. Veglia, Direct observation of the three regions in alpha-synuclein that determine its membrane-bound behaviour, *Nat. Commun.* 5 (2014) 3827.
- [26] M.E. Ward, E. Ritz, M.A. Ahmed, V.V. Bamm, G. Harauz, L.S. Brown, V. Ladizhansky, Proton detection for signal enhancement in solid-state NMR experiments on mobile species in membrane proteins, *J. Biomol. NMR* 63 (2015) 375–388.
- [27] M. Gustavsson, N.J. Traaseth, G. Veglia, Probing ground and excited states of phospholamban in model and native lipid membranes by magic angle spinning NMR spectroscopy, *Biochim. Biophys. Acta* 2012 (1818) 146–153.
- [28] T. Gopinath, S.E.D. Nelson, K.J. Soller, G. Veglia, Probing the conformationally excited states of membrane proteins via 1H-detected MAS solid-state NMR spectroscopy, *J. Phys. Chem. B* 121 (2017) 4456–4465.
- [29] G.A. Morris, R. Freeman, Enhancement of nuclear magnetic resonance signals by polarization transfer, *J. Am. Chem. Soc.* 101 (1979) 760–762.
- [30] S.R. Hartmann, E.L. Hahn, Nuclear double resonance in the rotating frame, *Phys. Rev.* 128 (1962) 2042–2053.
- [31] B. Buck, J. Zamoony, T.L. Kirby, T.M. DeSilva, C. Karim, D. Thomas, G. Veglia, Overexpression, purification, and characterization of recombinant Ca-ATPase regulators for high-resolution solution and solid-state NMR studies, *Prot. Exp. Purif.* 30 (2003) 253–261.
- [32] A.J. Shaka, J. Keeler, T. Frenkiel, R. Freeman, An improved sequence for broadband decoupling: WALTZ-16, *J. Magn. Reson.* 52 (1983) 335–338.
- [33] L. Bosman, P.K. Madhu, S. Vega, E. Vinogradov, Improvement of homonuclear dipolar decoupling sequences in solid-state nuclear magnetic resonance utilising radiofrequency imperfections, *J. Magn. Reson.* 169 (2004) 39–48.
- [34] F. Delaglio, S. Grzesiek, G.W. Vuister, G. Zhu, J. Pfeifer, A. Bax, NMRPipe: a multidimensional spectral processing system based on UNIX pipes, *J. Biomol. NMR* 6 (1995) 277–293.
- [35] T.D.G.a.D.G. Kneller, SPARKY 3.
- [36] M. Leskes, P.K. Madhu, S. Vega, Proton line narrowing in solid-state nuclear magnetic resonance: new insights from windowed phase-modulated Lee-Goldburg sequence, *J. Chem. Phys.* 125 (2006).
- [37] S. Paul, R.S. Thakur, M. Goswami, A.C. Sauerwein, S. Mamone, M. Concistre, H. Forster, M.H. Levitt, P.K. Madhu, Supercycled homonuclear dipolar decoupling sequences in solid-state NMR, *J. Magn. Reson.* 197 (2009) 14–19.
- [38] J. Li, Z.M. James, X.Q. Dong, C.B. Karim, D.D. Thomas, Structural and functional dynamics of an integral membrane protein complex modulated by lipid headgroup charge, *J. Mol. Biol.* 418 (2012) 379–389.
- [39] M. Gustavsson, N.J. Traaseth, C.B. Karim, E.L. Lockamy, D.D. Thomas, G. Veglia, Lipid-mediated folding/unfolding of phospholamban as a regulatory mechanism for the sarcoplasmic reticulum Ca²⁺-ATPase, *J. Mol. Biol.* 408 (2011) 755–765.
- [40] N.J. Baxter, M.P. Williamson, Temperature dependence of 1H chemical shifts in proteins, *J. Biomol. NMR* 9 (1997) 359–369.
- [41] M. Etzkorn, S. Martell, O.C. Andronesi, K. Seidel, M. Engelhard, M. Baldus, Secondary structure, dynamics, and topology of a seven-helix receptor in native membranes, studied by solid-state NMR spectroscopy, *Angew. Chem. (Int. Ed. Engl.)* 46 (2007) 459–462.
- [42] M. Renault, M.P. Bos, J. Tommassen, M. Baldus, Solid-state NMR on a large multidomain integral membrane protein: the outer membrane protein assembly factor BamA, *J. Am. Chem. Soc.* 133 (2011) 4175–4177.
- [43] J. Xu, R. Soong, S.C. Im, L. Waskell, A. Ramamoorthy, INEPT-based separated-local-field NMR spectroscopy: a unique approach to elucidate side-chain dynamics of membrane-associated proteins, *J. Am. Chem. Soc.* 132 (2010) 9944–9947.
- [44] R. Zhang, K.H. Mroue, A. Ramamoorthy, Hybridizing cross-polarization with NOE or refocused-INEPT enhances the sensitivity of MAS NMR spectroscopy, *J. Magn. Reson.* 266 (2016) 59–66.
- [45] K.N. Ha, M. Gustavsson, G. Veglia, Tuning the structural coupling between the transmembrane and cytoplasmic domains of phospholamban to control sarcoplasmic reticulum Ca²⁺-ATPase (SERCA) function, *J. Muscle Res. Cell Motility* 33 (2012) 485–492.
- [46] K.N. Ha, N.J. Traaseth, R. Verardi, J. Zamoony, A. Cembran, C.B. Karim, D.D. Thomas, G. Veglia, Controlling the inhibition of the sarcoplasmic Ca²⁺-ATPase by tuning phospholamban structural dynamics, *J. Biol. Chem.* 282 (2007) 37205–37214.